RESEARCH ARTICLE | NOVEMBER 21 2003

An efficient method for simultaneous measurement of the integrated reflectivity of crystals in multiple orders of reflection using the bremsstrahlung continuum from an x-ray tube and comparison of experimental results for mica with theoretical calculations ⊘

S. G. Lee; J. G. Bak; Y. S. Jung; M. Bitter; K. W. Hill; G. Hölzer; O. Wehrhan; E. Förster

Check for updates

CrossMark

View Online   Export Citation

Articles You May Be Interested In

X-ray imaging characteristics from a large spherically bent mica crystal (abstract)

Rev Sci Instrum (January 2001)

Coronary angiography using laser plasma sources: X-ray source efficiency and optimization of a bent crystal monochromator

Journal of Applied Physics (September 2001)

One-dimensional x-ray microscope for shock measurements in high-density aluminum plasmas

Rev Sci Instrum (January 1999)

AIP Publishing

An efficient method for simultaneous measurement of the integrated reflectivity of crystals in multiple orders of reflection using the bremsstrahlung continuum from an x-ray tube and comparison of experimental results for mica with theoretical calculations

S. G. Lee,[a] J. G. Bak, and Y. S. Jung
Korea Basic Science Institute, Yusung, Taejeon 305-333, Korea

M. Bitter and K. W. Hill
Princeton Plasma Physics Laboratory, Princeton, New Jersey 08543

G. Hölzer
X-Fab Semiconductor Foundries AG, Haarbergstrasse 61, 99097 Erfurt, Germany

O. Wehrhan and E. Förster
Friedrich-Schiller University, Jena, Germany

This article describes an efficient method for the simultaneous measurement of the integrated reflectivity of a crystal in multiple orders of reflection at a predefined Bragg angle by using the bremsstrahlung continuum from an x-ray tube in combination with an energy-sensitive detector. The technique is demonstrated with a mica crystal for Bragg angles of 43°, 47°, and 50°. The measured integrated reflectivity for Bragg reflections up to the 24th order is compared with theoretical predictions, which are also presented in this article. © *2003 American Institute of Physics.* [DOI: 10.1063/1.1619546]

I. INTRODUCTION

In a previous article,[1] Lee *et al.* described an efficient method of measuring the integrated reflectivity of a crystal by using the bremsstrahlung continuum from an x-ray tube in combination with an energy resolving x-ray detector. The method, which is called the ''bremsstrahlung method'' in this article, offers many advantages over the previously used technique and, due to the fact that it simultaneously determines the integrated reflectivity for all orders of reflection at a predefined Bragg angle, it is especially well suited for calibration of crystal spectrometers, which find wide applications in research and industry.

The measurements described in Ref. 1 were carried out with a mica crystal at a Bragg angle of 45° for Bragg reflections up to the 22nd order. Mica is distinctly different from most other crystals, since the integrated reflectivity for certain higher order Bragg reflections is larger than that of the lowest order. Because of these unusual properties, mica is particularly suitable for testing the bremsstrahlung method and validating of theoretical predictions. Calculations of the integrated reflectivity of mica for multiple orders of reflection at a predefined Bragg angle have recently been published by Hölzer *et al.*[2] These calculations are directly applicable to the experimental arrangement used in Ref. 1 and in this article.

In Ref. 1, theoretical predictions[2] of the integrated reflectivity of mica for Bragg angles in the range from 50° to 89° were extrapolated to a Bragg angle of 45°; these extrapo-

lations were found to be in good qualitative agreement with the experimental data. Furthermore, a quantitative agreement between the extrapolated values and the experimental data was obtained for a limited range of orders of reflection, which depended on the Bragg peak that was used for normalization of the observed integrated reflectivity to the expected value. However, with the comparison performed in Ref. 1, a quantitative agreement between experiment and theory could not be obtained for the entire spectrum of Bragg peaks. The *apparent* discrepancies between experiment and theory gave rise to questions about possible systematic errors in the measurement or interpretation of the data. It was also argued that the earlier-mentioned extrapolation of the theoretical predictions[2] might not be justified, since the Bragg angle of 45° corresponds to an energy near the *K*-absorption edge of aluminum, which is a constituent of mica.

In order to address these questions, we have performed additional measurements for Bragg angles of 43°, 47°, and 50°, which correspond to energies below and above the Al *K*-absorption edge, and have compared these experimental results with new theoretical calculations for these specific Bragg angles. The code used for these calculations is described in Ref. 3. We also repeated the measurement of the bremsstrahlung spectrum from the x-ray tube, taking great care to insure that the experimental arrangement of the detector with respect to the vacuum window was exactly the same as for the measurements of the Bragg peaks. These steps were taken in order to eliminate any experimental errors which might result from differences in absorption in air due a different length of the air gap between window and
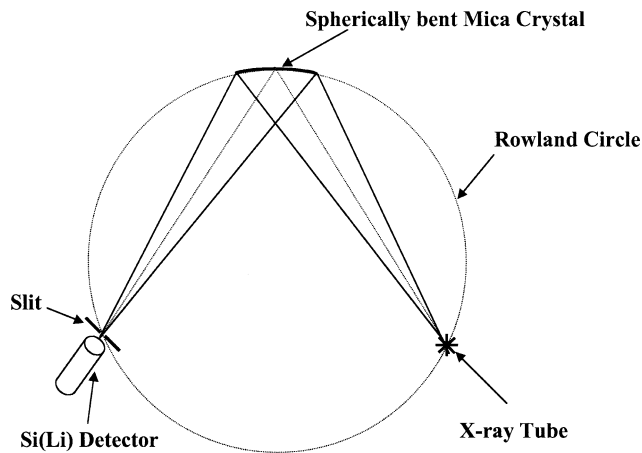
[a] Electronic mail: sglee@kbsi.re.kr

FIG. 1. Experimental arrangement.

FIG. 2. (Color) Overlay of two emission spectra from the x-ray tube. The spectra were obtained for slightly different experimental conditions.

detector. Moreover, we investigated the effects of weak fluorescent peaks on the measurement of the integrated reflectivity for certain orders of reflection. In the course of these investigations we discovered that the apparent discrepancies between theory and experiment reported in Ref. 1 were due to an error in the data analysis. After elimination of this error the experimental data are now in quantitative agreement with Hölzer's theory for the entire spectrum of Bragg peaks, except for the 12th and 18th order of reflection. Since these results are important for an experimental verification of the theory and a validation of our method, a detailed description of the experiments—including figures for each of the investigated Bragg angles—and data analysis is given in this article for future reference.

This article is organized as follows: The experimental arrangement is described in Sec. II. The experimental results are presented in Sec. III. The advantages of the bremsstrahlung method for measuring the integrated reflectivity are described in Sec. IV. Discussions are presented in Sec. V.

II. EXPERIMENTAL ARRANGEMENT

The experimental arrangement consisted of a spherically bent mica crystal, an x-ray tube, and energy-resolving Si(Li) detector, which were placed on the Rowland circle in the Johann configuration,[4] as shown in Fig. 1. The mica crystal had a radius of curvature of 1524 mm and a reflecting surface of 70 mm×17 mm. The x-ray tube was a small air-cooled device with a copper anode. Both the spherically bent mica crystal and the x-ray tube were mounted within a common vacuum chamber, while the Si(Li) detector was located outside the vacuum chamber behind a 20-μm-thick polypropylene foil, which served as a vacuum window. The foil was glued onto a blind flange with a borehole of 10 mm diameter. The sensitive area of the Si(Li) detector had a diameter of 5 mm and was covered by a protective 8-μm-thick beryllium foil. A copper plate with a 1 mm wide vertical slit was inserted between the detector and the polypropylene foil and placed on the Rowland circle. In order to minimize the attenuation of low-energy x rays in air, the inserted copper plate was in contact with the blind flange and the detector, so that the width of the air gap between the polypropylene foil and the detector was less than 2 mm. The slit width of
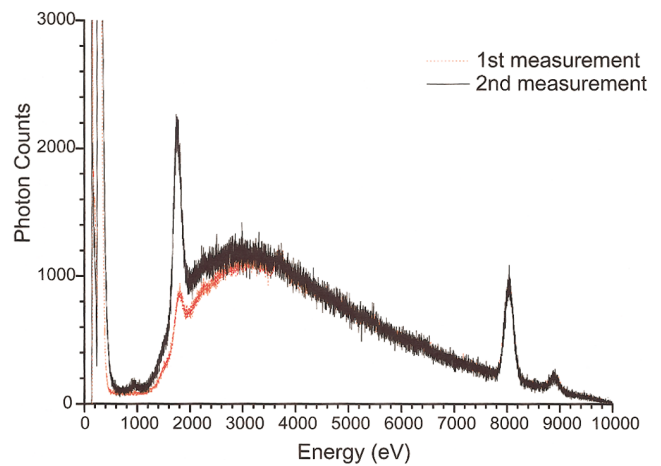
$w=1$ mm defined the angular resolution $\Delta\theta$ of the instrument. For measurements of the integrated reflectivity, w and $\Delta\theta$ were chosen to be larger than the Johann error[4] $(\Delta x)_J$ and the expected angular width $(\Delta\theta)_C$ from the intrinsic resolution and mosaic spread of the crystal. The Johann error was $(\Delta x)_J=0.28$ mm for our experimental conditions. The value of $(\Delta\theta)_C$ was derived from the theoretical values of the spectral resolving power $(\lambda/\Delta\lambda)_C$ for mica crystals given in Table 1 of Ref. 2. For a Bragg angle of 50°, the listed theoretical values are $(\lambda/\Delta\lambda)_C=1480$ and 4000 for reflection orders from 2 to 6 and reflection orders above 10, respectively. These values take into account a mosaic spread $\Delta\theta=1$ arc min. The resolving power of $(\lambda/\Delta\lambda)_C=1480$ corresponds to an angular width of $(\Delta\theta)_C=6.8\times10^{-4}$ or to a spatial resolution of $(\Delta x)_C=0.73$ mm at the position of the slit. The slit width of $w=1$ mm was therefore larger than the expected combined error of $(\Delta x)_J$ and $(\Delta x)_C$.

We note that the position of the x-ray tube is not important for the present measurements. In principle, the x-ray tube could be located at any position inside or outside the Rowland circle, as long as the x-ray emitting area of the anode is sufficiently large, so that the rays if they are considered as emanating from an imaginary source on the Rowland circle still subtend the entire area of the crystal. The size of the corresponding imaginary source on the Rowland circle and thus the energy resolution are solely determined by the width of the slit, which is placed on the Rowland circle in front of the detector.

III. EXPERIMENTAL RESULTS

A. Measurements of the bremsstrahlung continuum

Figure 2 shows an overlay of two bremsstrahlung spectra from the x-ray tube. The measurements were made at two different times and under slightly different experimental conditions, meaning that the distance between the Si(Li) detector and the polypropylene foil, which served as a vacuum window, was slightly different. However, in both cases, this distance was less than 2 mm. The spectrum shown by the *red dotted* line is from an earlier measurement and was used in

Ref. 1 for evaluation of the integrated reflectivity at a Bragg angle of $\Theta=45°$. The spectrum shown by the *black solid* line was obtained from a more recent measurement taken at the time when additional measurements of the integrated reflectivity for $\Theta=43°$, $47°$, and $50°$ were made. For the purpose of the overlay, the spectrum from the second measurement has been multiplied by a factor of 2.9. For both measurements of the bremsstrahlung continuum, the x-ray tube was placed in the line of sight of the Si(Li) detector. For the more recent measurement, the air gap between the detector and the polyethylene foil was exactly the same as for the measurements of the Bragg peaks at $\Theta=43°$, $47°$, and $50°$ and corresponded to the experimental arrangement described in Sec. II. The spectra shown in Fig. 2 consist of the Cu $K\alpha$ and Cu $K\beta$ lines at 8.040 and 8.905 keV, respectively, and a bremsstrahlung continuum which extends up to the operating voltage of 10 kV. The strong peak at 1.78 keV, which corresponds to the Si $K\alpha$ and Si $K\beta$ lines at 1.734 and 1.836 keV, respectively, is ascribed to fluorescent radiation in the Si(Li) detector. This peak was therefore not present in the radiation incident on the crystal during the measurements of the Bragg peaks. We infer from Fig. 2 that the spectra are in excellent agreement for energies in the range from 3.5 to 10 keV. This result leads to the important conclusion that, within this energy range, the experimental results from Ref. 1 and the present measurements are not affected by variations in the experimental conditions. At low energies the intensity is reduced due to attenuation by the polypropylene window, air gap, and beryllium foil on the detector. The intensity differences of the spectra for energies below 3.5 keV are due to the fact that the detector was closer to the vacuum window for the more recent measurement. The spectrum from the second measurement also shows a small peak at 0.94 keV representing the copper L lines.

B. Measurements of the integrated reflectivity

The integrated reflectivity was measured by the ratio of the intensity under a Bragg peak and the intensity of the incident bremsstrahlung continuum at the relevant energy. To facilitate a comparison between experiment and theory, the measured intensity ratio for one, arbitrarily chosen, Bragg peak was normalized to the theoretically predicted value for the integrated reflectivity. It is crucial for the evaluation of the Bragg peaks that the presence of spectral lines in the incident bremsstrahlung continuum and the presence of weak fluorescent lines, which are emitted from the constituent elements of the crystal and crystal holder, are taken into account. These effects must be investigated for each Bragg angle separately.

Figure 3 presents the experimental data obtained for a Bragg angle of 43°. The bremsstrahlung spectrum from the x-ray tube is shown in Fig. 3(a) and the energy-resolved spectrum of the Bragg reflected radiation from the 2nd up to the 20th order is shown in Fig. 3(b), and—on an expanded scale—in Fig. 3(c). The *black* vertical lines represent the calculated positions for the Bragg peaks. The *red* dotted vertical lines designate the energies of the spectral lines of Cu and Si. The Cu lines, which originate from the anode, are
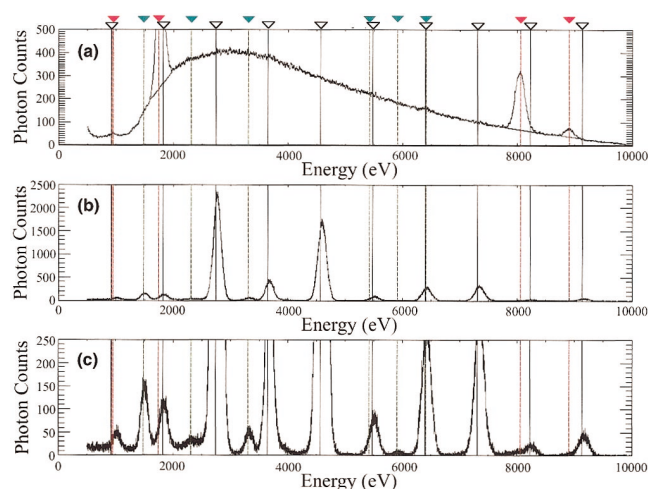

FIG. 3. (Color) Raw spectral data. (a) The emission spectrum from the x-ray tube. (b) and (c) The Bragg reflected radiation from the mica crystal for $\Theta=43°$ on different scales. The black lines mark the calculated positions of the Bragg peaks. The red lines indicate the energies of Cu lines, which are emitted from the anode, and the Si lines produced in the Si(Li) detector. The green lines mark the energies of weak fluorescent lines from elements in the crystal and crystal holder. The triangles on top of the figure were introduced to improve legibility of the various lines.

present in the incident radiation, and the Si lines are produced in the detector. The *green* dotted vertical lines designate the energies of small additional peaks, which are not present in the incident bremsstrahlung spectrum and whose positions are independent of the Bragg angle. These peaks are due to fluorescent radiation from the crystal and crystal holder and correspond to the $K\alpha$ and $K\beta$ lines of Al, S, K, Mn, Cr, and Fe. The strongest lines are the $K\alpha$ and $K\beta$ lines of Al and K at 1.5 and 3.3 keV. A significant contribution to the Al $K\alpha$ line originates from the crystal holder, which was fabricated out of aluminum. Cr and Fe are major constituents of mica crystals. The fluorescent peaks from S, Mn, Cr, and Fe are much weaker than those of Al and K. These fluorescent peaks can interfere with the measurements of the integrated reflectivity if they coincide with the position of Bragg peaks and if the Bragg peaks are small. The existence of such interferences must be carefully checked for each Bragg angle. Figure 3(c) also shows the presence of some detector noise at the lowest energies. This detector noise affects the evaluation of the integrated reflectivity for the second and, to a lesser extent, fourth order of reflection.[5]

The observed width and shape of the Bragg peaks are determined by the energy resolution of the Si(Li) detector of 155 eV full width at half maximum (FWHM). However, the range of energies which contribute to each Bragg peak is much narrower and of the order of a few electron volts, since the resolution of the crystal spectrometer is $\lambda/\Delta\lambda=1500$–4000, depending on the Bragg angle. We may therefore conclude that, for $\Theta=43°$, the observed Bragg peaks are well separated from any spectral lines—except for the Bragg peak of the 18th order, which is very close to the Cu $K\alpha$ line. The Cu $K\alpha$ line may therefore interfere with the measurement of the integrated reflectivity for the 18th order.

The intensity under each Bragg peak was determined from a least squares fit of a Gaussian with a FWHM of 155
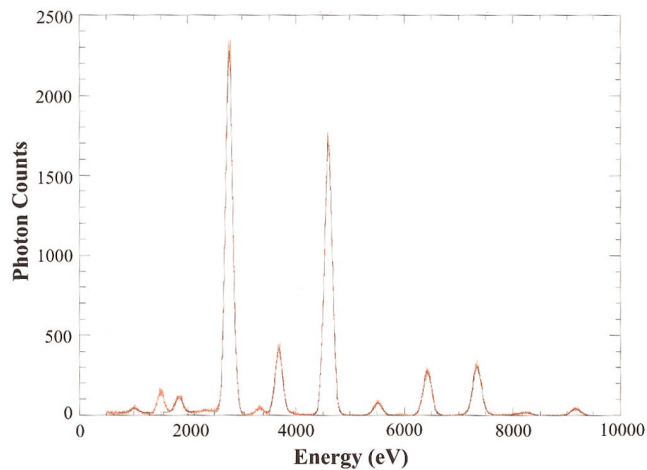
FIG. 4. (Color) Observed Bragg peaks (*in red*) for $\Theta=43°$ and least squares fits of Gaussians (*black solid lines*) with a FWHM of 155 eV corresponding to the energy resolution of the Si(Li) detector.
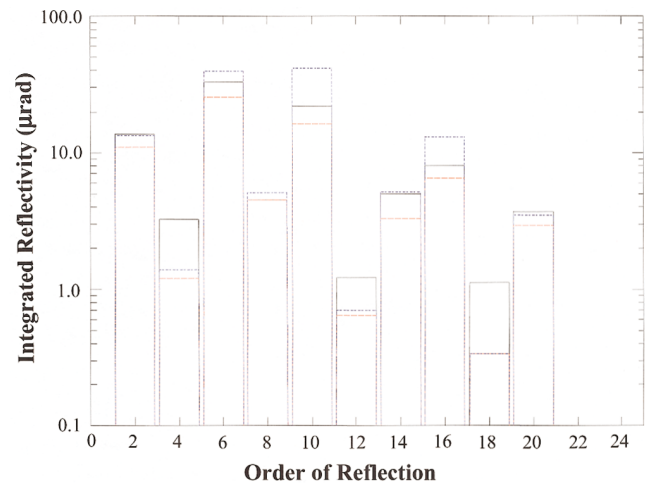

FIG. 5. (Color) Comparison of the experimental and predicted values for the integrated reflectivity for $\Theta=43°$. The experimental values are shown by the *black solid lines*, and the theoretical values from the dynamic theory and the predicted kinematic limit are shown by the *red* and *blue* lines, respectively. To facilitate the comparison, the experimental values have been normalized by setting experimental value for the 8th order of reflection equal to the value predicted by the dynamical theory.

eV as shown in Fig. 4. An important point of the data analysis—which was overlooked in Ref. 1 and which was the cause for the "apparent" discrepancies between the experiment and theory—is that the width of the energy interval ΔE that contributes to a Bragg reflection varies in proportion to the energy E of the Bragg peak according to the equation, $\lambda/\Delta\lambda=\Delta E/E=\Delta\Theta/\tan(\Theta)=$constant, since the measurements were performed at a constant Bragg angle Θ and a constant $\Delta\Theta$. For an evaluation of the integrated reflectivity, the intensity under a Bragg peak must be divided by the intensity, $I(E)\,\Delta E$, of the incident bremsstrahlung, where $I(E)$ is the bremsstrahlung intensity at the energy E, and ΔE is proportional to E. The error in the data analysis of Ref. 1 was that ΔE was kept constant for all the Bragg peaks independent of their energies.

Another important point for the data analysis is that, in the vicinity of a spectral line, one must take the interpolated intensity of the bremsstrahlung spectrum [see Fig. 3(a)], rather than the intensity including the spectral line, if the separation between the center positions of the Bragg peak and the spectral line is larger than ≈ 5 eV, since the widths of

spectral lines ($\lesssim 5$ eV) are much smaller than the apparent line profiles, which are only an artifact due to the finite resolution of the Si(Li) detector.

Following these procedures, we have obtained the experimental values for the integrated reflectivity, which are shown in Fig. 5 and Table I together with the theoretical predictions from Ref. 2. These theoretical predictions include the value from the dynamic theory[6,7] and the kinematic limit. The experimental results have been normalized by setting the experimental value for the 8th order of reflection equal to the corresponding dynamic value of 4.4762 μrad from the theory.[2] The experimental values are shown by the *black* solid lines, and the theoretical values from the dynamic theory and the kinematic limit are shown by the *red* and *blue* lines, respectively. We infer from Fig. 5 that—except for the 12th and 18th order of reflection—the experimental values are between (or close to) the theoretically predicted values of the dynamic theory and kinematic limit.
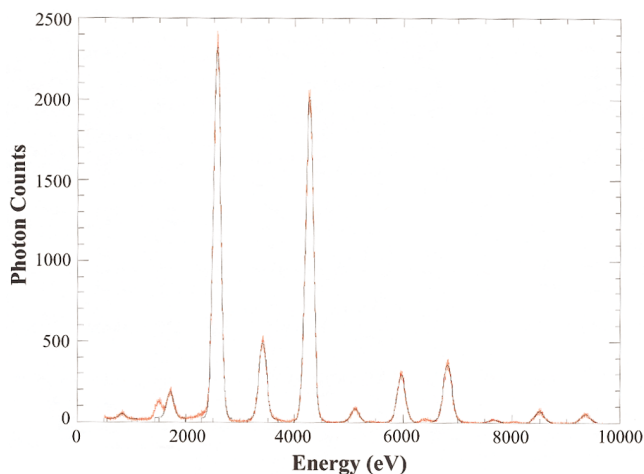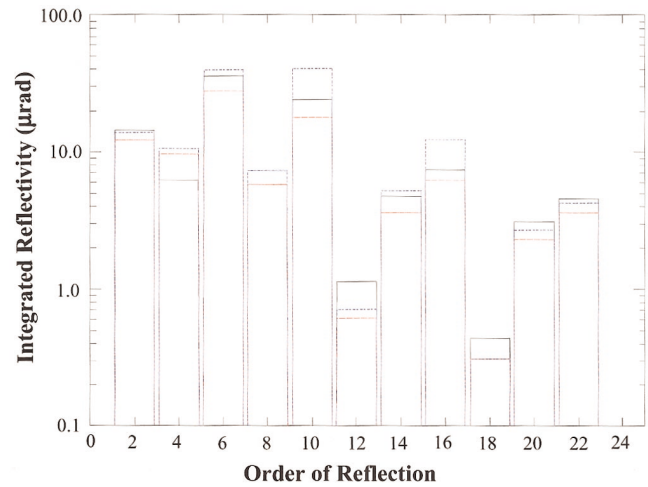
TABLE I. Theoretical and experimental values for the integrated reflectivities of a mica crystal with a radius of curvature of 1524 mm for Bragg angles of 43°, 47°, 50°, and 45° in multiple orders of reflection. Columns a, b, and c represent the integrated reflectivity from the dynamic theory, the kinematic limit, and experimental values in units of μrad, respectively. The experimental values for the 8th order of reflection (*) have been normalized to the predicted values from the dynamic theory.

Order of reflection	$\theta=43°$			$\theta=47°$			$\theta=50°$			$\theta=45°$		
	a	b	c	a	b	c	a	b	c	a	b	c
2	10.99	13.49	13.89	12.2	13.8	14.28	13.41	14.33	23.01	11.57	13.59	20.40
4	1.18	1.39	3.30	9.7	10.6	6.28	14.77	17.20	11.60	5.99	6.79	5.07
6	25.80	39.83	33.40	27.8	39.9	36.27	29.06	41.46	40.47	26.35	39.60	35.29
8	4.48	5.08	4.48*	5.8	7.3	5.8*	6.52	7.99	6.52*	5.08	6.33	5.08*
10	16.31	41.38	22.14	17.9	40.7	24.04	20.02	42.28	26.53	16.85	41.25	24.04
12	0.63	0.69	1.23	0.6	0.7	1.12	0.61	0.69	1.19	0.61	0.68	1.19
14	3.25	5.13	5.04	3.6	5.2	4.77	3.27	5.56	5.04	3.11	5.16	5.18
16	6.50	12.95	8.03	6.2	12.3	7.48	5.60	13.80	8.03	5.98	12.94	8.96
18	0.32	0.32	1.12	0.3	0.3	0.43	0.34	0.35	0.53	0.32	0.32	0.68
20	2.94	3.48	3.73	2.3	2.7	3.06	2.32	3.68	3.94	2.80	3.47	2.94
22				3.6	4.2	4.59	3.38	6.75	26.53	4.57	6.37	6.17
24							2.46	3.38	2.88			
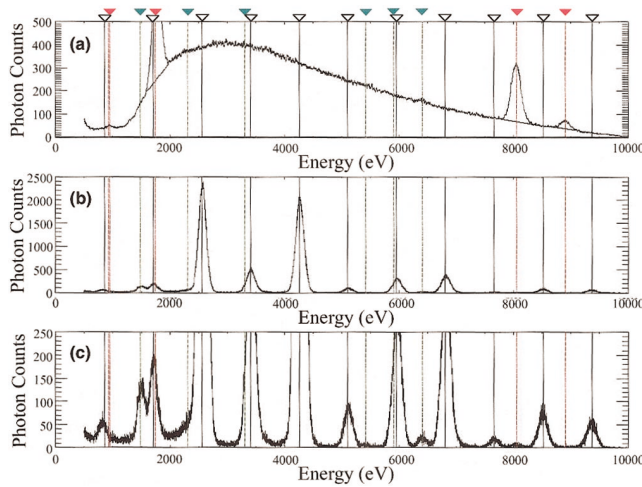
FIG. 6. (Color) Raw spectral data for $\Theta=47°$, similar to Fig. 3.

FIG. 8. (Color) Comparison of the experimental and predicted values for the integrated reflectivity for $\Theta=47°$, similar to Fig. 5.

The observed deviation for the 18th order of reflection may be due to an interference with the Cu $K\alpha$ line. The experimental values for the integrated reflectivity of the 2nd and 4th order of reflection are less certain, since the evaluation of these Bragg peaks is affected by the elevated background at low energies due to detector noise and by a small fluorescent peak at 2.3 keV, which may be ascribed to the L lines of high-Z elements, such as Mo, and since the (measured) intensity of the incident bremsstrahlung spectrum at the position of the 2nd order peak is very small. However, the experimental uncertainties for the 4th order are smaller than those for the 2nd order. The experimental values for the 6th up to the 20th order, which fall into the energy range from 3 to 10 keV, should be very reliable—with exception of the experimental value for the 18th order, which may be impaired by the vicinity of the Cu $K\alpha$ line.
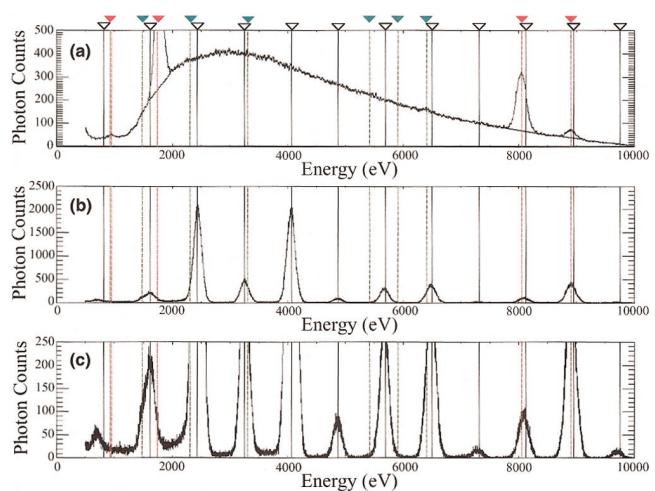
The same general comments apply to Figs. 6–11, which represent the results for the Bragg angles 47° and 50°. There are a few additional observations. The fluorescent peak at 3.3 keV from potassium (K) interferes with the 8th order Bragg peak for the Bragg angles of 47° and 50°, requiring a small correction for the measured integrated reflectivity for the 8th

order. Moreover, for the Bragg angle of 50°, there is an interference between the Bragg peak of the 22nd order and the Cu $K\alpha$ line. Dividing by the extrapolated bremsstrahlung spectrum is not justified here, since the 22nd order Bragg peak is too close to the Cu $K\alpha$ line and since it is difficult to determine the exact contribution from the Cu $K\alpha$ line. The experimental value for the integrated reflectivity of the 22nd order is therefore not reliable.

Also shown in Fig. 12 are the corrected experimental values for the integrated reflectivity for the Bragg angle of 45°. The raw data for the bremsstrahlung spectrum and Bragg peaks were already shown in Figs. 2 and 3 of Ref. 1.

We note that the experimental values for the integrated reflectivity of the 12th and 18th order are higher than the kinematic limit for all the investigated Bragg angles. Since—for the Bragg angles of 47° and 50°—the 18th order Bragg peak is well separated from the Cu $K\alpha$ line, an interference of the Cu $K\alpha$ line with the 18th order Bragg peak can be excluded for these Bragg angles. We are therefore led to conclude that there is still a systematic difference between the experimental results and the theoretical predictions for the 12th and 18th order of reflection. The experimental re-

FIG. 7. (Color) Observed Bragg peaks (*in red*) and least squares fits of Gaussians (*black solid lines*) for $\Theta=47°$.

FIG. 9. (Color) Raw spectral data for $\Theta=50°$, similar to Fig. 3.
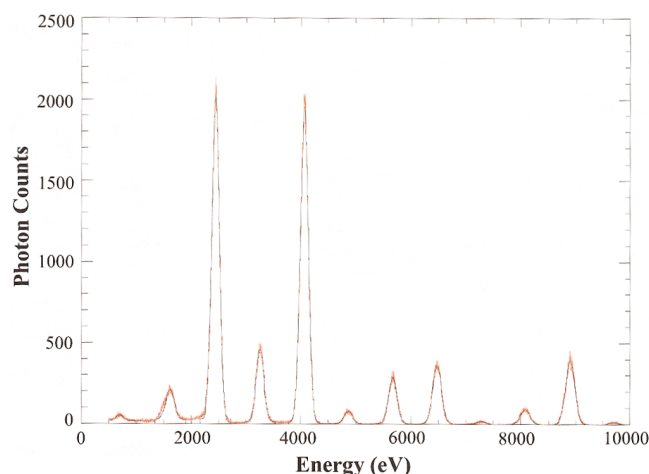
FIG. 10. (Color) Observed Bragg peaks (*in red*) and least squares fits of Gaussians (*black solid lines*) for $\Theta=50°$.

FIG. 12. (Color) Comparison of the experimental and predicted values for the integrated reflectivity for $\Theta=45°$, similar to Fig. 5.

sults and theoretical predictions for the integrated reflectivity for all the investigated Bragg angles are listed in Table I.

IV. ADVANTAGES OF THE BREMSSTRAHLUNG METHOD

The bremsstrahlung method of measuring integrated reflectivity described in this article offers many advantages over the commonly used (standard) procedure, which is illustrated in Fig. 7 of Ref. 2. The previous technique employs monochromatic radiation of characteristic x-ray lines, such as the Cu $K\alpha$ line at 0.154 056 nm and the Mo $K\alpha$ line at 0.070 93 nm, from the anode of an x-ray tube. This line radiation is separated from the bremsstrahlung continuum by Bragg reflection from a monochromator crystal and then directed onto the sample crystal. The cross section of the incident monochromatic beam and the corresponding x-ray spot on the sample crystal is about 1 mm^2. The sample crystal is rotated through a small range of Bragg angles around the Bragg angle for which the maximum reflectivity is expected,
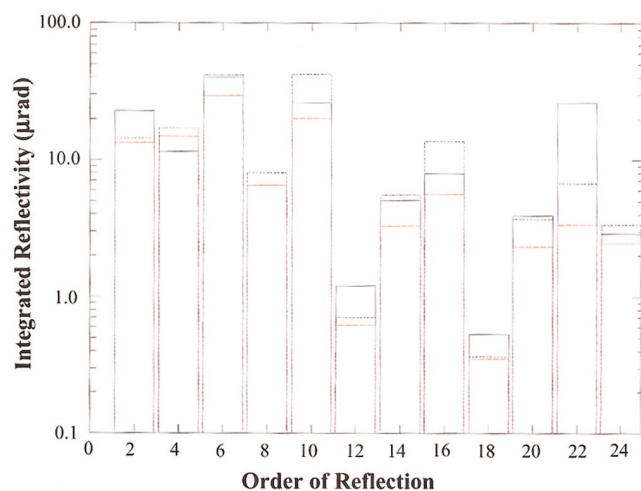

FIG. 11. (Color) Comparison of the experimental and predicted values for the integrated reflectivity for $\Theta=50°$, similar to Fig. 5.
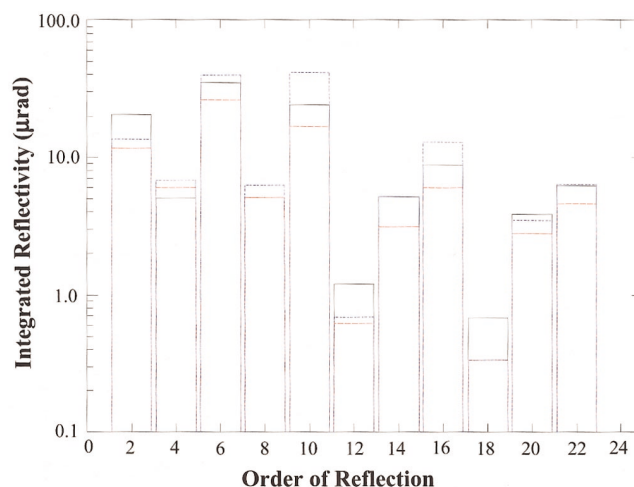
and the reflected x-ray intensity is monitored with an x-ray detector, e.g., a scintillator and photomultiplier tube, which is only used as a photon counter.

This procedure is very tedious and time consuming and it can be readily used only for a limited number of x-ray energies, those corresponding to the $K\alpha$ lines of available anodes. In fact, a change of the energy requires the installation of a different anode in the x-ray tube. Moreover, the measurement of each Bragg reflection requires a new alignment of the sample crystal and detector and subsequent scanning of the sample crystal through a range of Bragg angles. We also point out that the standard procedure provides the integrated reflectivity for the different orders of reflection for a *predetermined energy*, namely, the energy of the characteristic x-ray lines from the anode, and not for a *predetermined Bragg angle*, which is of more immediate interest for the calibration of a crystal spectrometer.

In contrast to the commonly used technique, the bremsstrahlung method can provide the integrated reflectivity for *any* x-ray energy since the incident radiation consists of the bremsstrahlung continuum, instead of the characteristic line radiation. The bremsstrahlung method is therefore independent of the material of the anode and can be used with any x-ray tube. The upper limit of the energy range of the bremsstrahlung continuum can be simply adjusted by changing the high voltage applied to the x-ray tube.

Since the bremsstrahlung method yields the integrated reflectivity for different orders of reflection simultaneously at a predetermined Bragg angle with one fixed experimental arrangement, it is very well suited for an *in situ* calibration of a crystal spectrometer, which is usually set up for a certain Bragg angle. The relative values of the integrated reflectivity obtained for the different orders of reflection are very accurate and are not affected by fluctuations in the x-ray intensity from the x-ray tube, since all the Bragg peaks are measured simultaneously. It is therefore not necessary to monitor the x-ray flux from the x-ray tube. Moreover, the integrated reflectivity is measured for a narrow energy interval of a few electron volts that corresponds to the spectral resolution of the spectrometer, while with the commonly used technique

the energy interval is typically about 20–40 eV wide, since it includes both the characteristic $K\alpha$ and $K\beta$ lines from the anode.

Further advantages of the bremsstrahlung method are due to the fact that the entire crystal is illuminated by the x-ray tube. The throughput, which is proportional to the illuminated area of the crystal, can therefore be orders of magnitude larger than that of the commonly used technique, where the area of the x-ray spot on the crystal is typically only about 1 mm^2. The bremsstrahlung method also yields the integrated reflectivity of the entire crystal, whereas the commonly used procedure yields the integrated reflectivity from only a small, about 1 mm^2, area of the crystal. To measure the integrated reflectivity of the different orders of reflection from the entire crystal with the standard technique would be very tedious (or practically impossible), since it requires scanning of the incident monochromatic x-ray beam over the entire crystal surface. Moreover, this process would have to be repeated for the Bragg reflections of each order.

Another advantage of the bremsstrahlung method is due to the fact that it uses the x-ray flux directly from an x-ray tube, rather than x rays of greatly reduced intensity diffracted from a preselector crystal, as is the case with the standard technique. Therefore, much lower power can be used on the x-ray tube. This fact has two favorable implications: (1) much cheaper and smaller air-cooled x-ray tubes can be used, rather than expensive, heavy, bulky water-cooled tubes, which are needed for the standard procedure; and (2) radiation shielding and personnel radiation protection requirements are greatly reduced. This lower flux requirement allows, for instance, the use of "*homemade*," low-power, and windowless, x-ray tubes, which can be directly connected to the vacuum of the spectrometer chamber. Such x-ray tubes are of particular interest for the investigation of low-energy x rays below 1 keV. We point out that commercially available high-power x-ray tubes are usually manufactured with vacuum windows, which severely attenuate the x-ray intensity at energies below 1 keV. We also point out that the accessible energy range can be extended from 0.2 to 100 keV with the use of windowless Si(Li) detectors for low x-ray energies and Ge-diode detectors for high x-ray energies.

With the bremsstrahlung method it is also possible to observe, in addition to the Bragg peaks, the fluorescent radiation from the constituents of the material under investigation. This possibility will be of interest for an *in situ* analysis of structures, such as multilayer structures, during the manufacturing process.

V. DISCUSSION

In an effort to verify our earlier results from Ref. 1, additional measurements of the integrated reflectivity have been performed at Bragg angles of 43°, 47°, and 50°. Special care was taken to assure the uniformity of the experimental conditions for measurements of the Bragg peaks and the incident bremsstrahlung continuum. Moreover, corrections for contributions from fluorescent peaks were made, where necessary. In the course of these investigations, we discovered that the apparent discrepancies between theory and experiment—that had been reported in Ref. 1—were actually due to an oversight in the data analysis. After correcting for this oversight we now obtain very good agreement between theory and experiment for the entire spectral range, except for the 12th and 18th orders of reflection. The experimental results suggest that the theory does not yet adequately describe these orders of reflection. A detailed description of the experimental results and data analysis has been given in this article for future reference.

[1] S. G. Lee, J. G. Bak, Y. S. Jung, M. Bitter, K. W. Hill, O. Wehrhan, and E. Förster, Proc. SPIE **4501**, 177 (2001).
[2] G. Hölzer *et al.*, Phys. Scr. **57**, 301 (1998).
[3] G. Hölzer, O. Wehrhan, and E. Förster, Cryst. Res. Technol. **33**, 555 (1988).
[4] H. H. Johann, Z. Phys. **69**, 185 (1931).
[5] Here, we adopt the characterization of mica crystals from [G. Hölzer *et al.*, Phys. Scr. **57**, 301 (1998)], assuming a lattice constant of $d = 19.9149$ Å (private communication by Dr. A. Ya. Faenov), where even orders of reflection are allowed and odd orders of reflection are forbidden due to crystal symmetry. In the literature, the value of 19.9149 Å is often given as the value of the $2d$ spacing and no distinction is made between odd and even orders of reflection, i.e., all orders of reflection are allowed.
[6] D. Taupin, Bull. Soc. Fr. Mineral. Cristallogr. **87**, 469 (1964).
[7] Z. G. Pinsker, *Dynamical Scattering of X-Rays in Crystals* (Springer, Berlin, 1979).